Earth and Planetary Science Letters 469 (2017) 15–26

Contents lists available at ScienceDirect

Earth and Planetary Science Letters

www.elsevier.com/locate/epsl

Surface vitrification caused by natural fires in Late Pleistocene wetlands of the Atacama Desert

Pierrick Roperch [a,*], Jérôme Gattacceca [b], Millarca Valenzuela [c], Bertrand Devouard [b], Jean-Pierre Lorand [d], Cesar Arriagada [e], Pierre Rochette [b], Claudio Latorre [f,g], Pierre Beck [h]

[a] Géosciences Rennes, CNRS–INSU, Université de Rennes 1, Rennes, France
[b] CNRS, Aix Marseille Univ., IRD, Coll France, CEREGE, Aix-en-Provence, France
[c] Instituto de Astrofísica, P. Universidad Católica de Chile, Av. Vicuña Mackenna 4860, Santiago, Chile
[d] Laboratoire de Planétologie et Géodynamique, CNRS UMR 6112, Université de Nantes, 2 Rue la Houssinière, 44322, Nantes, France
[e] Departamento de Geología, Facultad de Ciencas Físicas y Matemáticas, Universidad de Chile, Plaza Ercilla 803, Santiago, Chile
[f] Centro UC del Desierto de Atacama and Departamento de Ecología, Pontificia Universidad Católica de Chile, Alameda 340, Santiago, Chile
[g] Institute of Ecology & Biodiversity (IEB), Santiago, Chile
[h] Institut de Planétologie et d'Astrophysique de Grenoble (IPAG), 414, Rue de la Piscine, Domaine Universitaire, 38400 St-Martin d'Hères, France

ARTICLE INFO

Article history:
Received 16 November 2016
Received in revised form 29 March 2017
Accepted 3 April 2017
Available online 21 April 2017
Editor: M. Bickle

Keywords:
silicate glass
airburst
wetland
pyrometamorphism
Younger Dryas
Atacama Desert

ABSTRACT

We describe extended occurrences of unusual silicate glass surface layers from the Atacama Desert (Chile). These glasses, found near the town of Pica at four localities separated by up to 70 km, are neither fulgurites, nor volcanic glasses, nor metallurgical slags related to anthropic activity, but show close similarities to other glasses that have been previously attributed to large airbursts created by meteoroids entering the Earth's atmosphere. The glasses are restricted to specific Late Pleistocene terrains: paleo-wetlands and soils rich in organic matter with SiO_2-rich plant remains, salts and carbonates. ^{14}C dating and paleomagnetic data indicate that the glasses were formed during at least two distinct periods. This rules out the hypothesis of a single large airburst as the cause of surface melting. Instead, burning of organic-rich soils in dried-out grassy wetlands during climate oscillations between wet and dry periods can account for the formation of the Pica glasses. Large oases did indeed form in the hyperarid Atacama Desert due to elevated groundwater tables and increased surface discharge during the Central Andean Pluvial Event (roughly coeval with the Mystery interval and Younger Dryas). Finally, we discuss the implications of our results for the other surface glasses previously attributed to extraterrestrial events.

1. Introduction

Impact glasses are a common feature associated with many terrestrial impact structures (French and Koeberl, 2010). Most meteoroids disintegrate during their entry into the Earth's atmosphere. The Chelyabinsk (Brown et al., 2013) and Tunguska (Svetsov and Shuvalov, 2008) airbursts were the most recent and best described examples of strong airbursts. These events had no significant thermal effects on the ground. However, numerical modeling suggests that the energy released by the largest low-altitude airbursts of cosmic bodies (asteroids, comets) during their entry into the Earth's atmosphere could have catastrophic effects (Boslough and Crawford, 2008). Indeed, a large comet airburst has even been proposed to have caused Younger Dryas cooling (Firestone et al., 2007; Bunch et al., 2012; Wittke et al., 2013), an explanation that has garnered considerable opposition (see Surovell et al., 2009; Pigati et al., 2012; Boslough et al., 2013). Melting of the soil surface by radiation from large airburst has also been proposed (Wasson, 2003; Boslough and Crawford, 2008) to explain the formation of some anomalous silicate glasses like the Libyan Desert Glass (Barrat et al., 1997; Kramers et al., 2013). Other examples include Miocene glass deposits found in the Argentine pampas (Schultz et al., 2004) as well as Pleistocene scoriaceous glasses from Australia (Haines et al., 2001) (Edeowie glass, age 0.6 to 0.8 Ma) and northern Africa (Osinski et al., 2007, 2008) (Dakhleh glass, age 145 ± 19 ka). French and Koeberl (2010) point out that it is often difficult to ascribe an impact origin to such glasses, which closely resemble non-impact glasses such as fulgurites, volcanic glasses or even metallurgical slags. The origin and mechanism of formation of these glasses is thus strongly debated. Hence, proving

* Corresponding author.
E-mail address: pierrick.roperch@univ-rennes1.fr (P. Roperch).

http://dx.doi.org/10.1016/j.epsl.2017.04.009
0012-821X/

Fig. 1. Satellite image (from Google Earth) of the northern Atacama desert with locations of the Pica Glass fields: Puquio de Nuñez (PN), Quebrada de Chipana (QC), Quebrada de Guatacondo (QG) and NW of the town of Pica (NWP). Contour line spacing is 500 m. The Salar de Coipasa (SC) and Salar de Uyuni in the Bolivian Altiplano highlight the extent of the late Pleistocene paleolake Tauca.

or disproving the impact origin of these glasses has implications for estimating the flux of airburst producing bolides to the Earth.

Massive glass blocks (called Pica Glass or PG in the following) were recently discovered (Blanco and Tomlinsson, 2013) lying on the surface along the eastern margin of the Tamarugal–Llamara basin in the Atacama Desert, Chile (Fig. 1). They were interpreted as the consequence of a major airburst (Blanco and Tomlinsson, 2013). We present field and petrographic observations, as well as ^{14}C dating to further constrain their origin. Paleomagnetism is used to complement ^{14}C dating, as it can be used to test the synchroneity of the glass formation at the different locations. Indeed the paleomagnetic study of the PG and underlying baked clays constrain the intensity and direction of the geomagnetic field at the time of glass formation. Moreover paleomagnetism also constrains the temperature reached by these clays. Finally it is also a test for the origin of the PG as fulgurites. Indeed, lighting strikes create strong magnetic fields (>100 mT) that result in specific remagnetization of the surrounding rocks (Graham, 1961).

2. Geology and field observations

Dark green, vesiculated (up to 50 vol% vesicles) and irregularly shaped, tabular glassy bodies occur scattered on the surface of the Atacama desert at several localities roughly aligned in a North–South direction and separated by more than 70 km. Here, we will only discuss observations made at four localities (Puquio de Nuñez, Quebrada de Chipana, Quebrada de Guatacondo, and NW of Pica) (Fig. 1). Individual blocks up to 50 cm wide and 1 to 30 cm thick are scattered over areas up to 1 km^2 in extent (Figs. 2, 3). Their glassy texture demonstrates high temperature melting and quenching.

At the site called “Puquio de Nuñez”, north of the small oasis of Puquio de Nuñez (Fig. 2a), the glasses are distributed over a ~2 km^2, almost flat surface (elevation 1200–1210 m) of late Pleistocene paleo-wetlands deposits (Blanco and Tomlinsson, 2013; Blanco et al., 2012) covering a Miocene tectonic flexure on the western border of the basin, which is filled by Neogene sediments (Nester, 2008). Glass blocks are distributed unevenly and locally concentrated over surfaces up to several tens of meters across (Fig. 2b). Such concentrations are more frequent on tops of small ridges or ground mounds. Glasses are also found in the sandy soil covered by a ~10 cm thick layer of sand (Fig. 2e). Some samples present a striated surface, grooves and tube-shaped cavities that are remnants of plants such as twigs and roots (Fig. 4; Supplementary Fig. S1).

Puquio de Nuñez oasis is presently mostly artificial (i.e. it has been dug out) and extends only for a few tens of meters. Water wells, drilled ~300 m to the east of Puquio de Nuñez, penetrate the water table located a few meters below the present-day arid surface. A sub-surface fault probably impedes the flow of ground water to the west bringing it close to the surface in this area. The Puquio de Nuñez area was from time to time a more humid area in the past (Blanco et al., 2012), when the water table reached its highest level.

At Quebrada de Chipana, located ~35 km south of Puquio de Nuñez, glasses are found in two separated fields (Fig. 3a). To the west, glassy blocks of variable size up to 50 cm thick are scattered at the surface (Fig. 3b, c). To the east, glassy blocks are found directly overlying red clay sediments that correspond to an old terrace with an overbank clay deposit along the intermittent stream of Quebrada de Chipana (Fig. 3d, e, f). The clay deposit has been partly eroded or covered by younger deposits but the best remains can be observed *in situ* with a thickness of about 10 to 30 cm (Fig. 3f). Although erosion has broken up most of the silicate glasses from the baked clays, we can still find evidence of several glasses in their *in situ* position just above the clay layer. Silicified plant twigs and imprints are common in the baked clays (Supplementary Fig. S1). A 20–30 cm thick layer of buried plant material is frequently associated with the glasses (Fig. 4a; Supplementary Fig. S1). Fossil plants, currently composed of silica (50%) and carbonates (20%) with almost no residual organic matter, are often mixed with or underlie the baked clays or the glasses (Fig. 4c, d; Supplementary Fig. S1).

At Quebrada de Guatacondo, most of the glasses are found north of the Quebrada (intermittent stream), a few meters above the present-day base level of the stream. The glass layer is more discontinuous than at the two previous sites (Puquio de Nuñez, Quebrada de Chipana). Glasses are sometimes found above and below a 10–20 cm thick white layer composed mainly of burnt but not melted silicified plant remains (Supplementary Fig. S1). Glasses above the white layer consist mainly of melted silicified plant twigs. The largest glassy blocks, up to 30 cm thick, are found within the soil below the white layer. Plant remains and plant imprints are also observed in the glasses formed within the soil (Supplementary Fig. S1c, d).

Abundant *in situ* glasses are found about 9 km to the northwest of the Pica town. The glasses are spread over about 1 km at the base of the southern and eastern edges of low-lying hills. These hills, related to a tectonic fault (Blanco et al., 2012; Blanco and Tomlinsson, 2013), limit a paleo-wetland deposit to the west with a mean elevation of 1100 m. Burnt soils without glasses are also observed on the surface in the same general area. Isolated glassy blocks also occur within the town of Pica itself, but these blocks could have been transported from their original location.

At all localities, most glasses contain plant imprints or silicified plant remains (Fig. 4; Supplementary Fig. S1).

3. Petrography, mineralogy, geochemistry

3.1. Samples and methods

Microscope observations were made on polished thin sections in transmitted light and reflected light. The samples were then observed with scanning electron microscopes (JEOL JSM 7100F with energy dispersive x-ray spectroscopy (Oxford EDS/EBSD) at University of Rennes1, and Hitachi S-3000N SEM, at CEREGE, operated at 15 kV, and fitted with a Bruker X-Flash detector and SPIRIT EDS system).

Whole-rock chemical analyses for 13 samples of PG, one sample of silicified plants and one soil sample were acquired at the

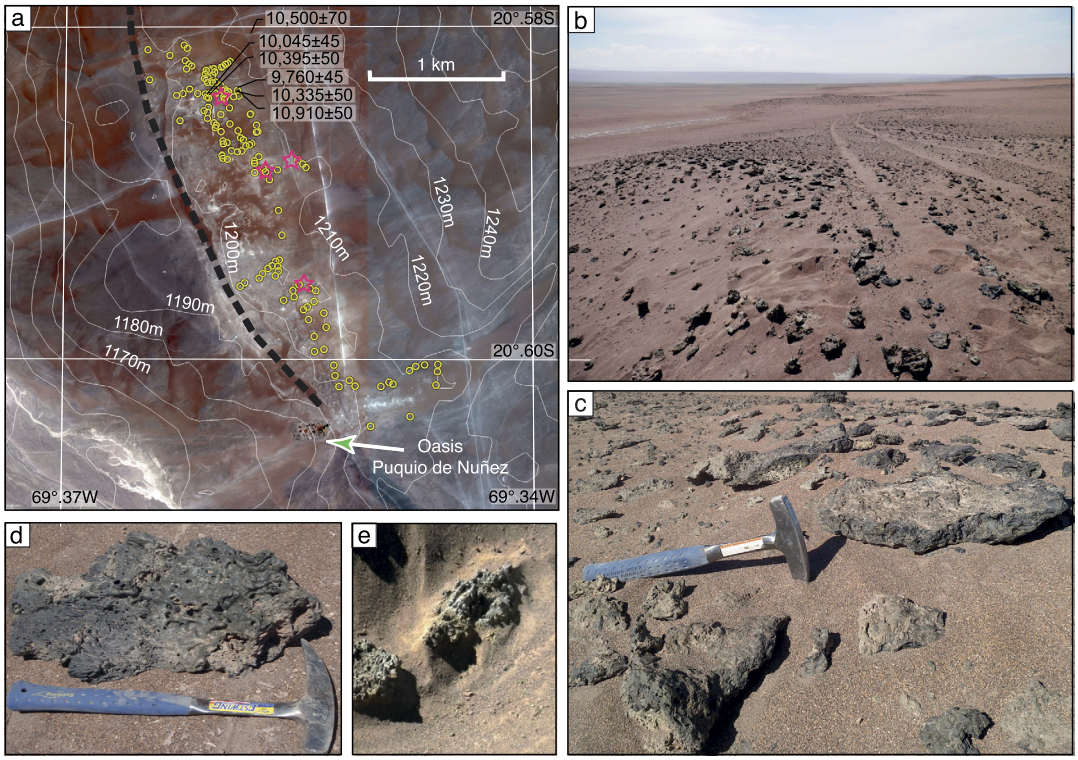

Fig. 2. Field observations at Puquio de Nuñez. (a) Satellite image (from Google Earth) showing locations where glasses were observed (yellow dots), ^{14}C ages and main paleomagnetic sampling (red stars). Elevation with contour line spacing of 10 m. The dashed thick black line indicates a tectonic flexure. (b, c) Field images showing outcrops with samples of dark glasses partially covering the ground. (d) Field photograph of a vitreous, dark green, vesiculated and irregularly shaped tabular Pica glass block on the surface. (e) Field photograph of a glass sample within the soil under a 5–10 cm thick layer of sand. (For interpretation of the references to color in this figure legend, the reader is referred to the web version of this article.)

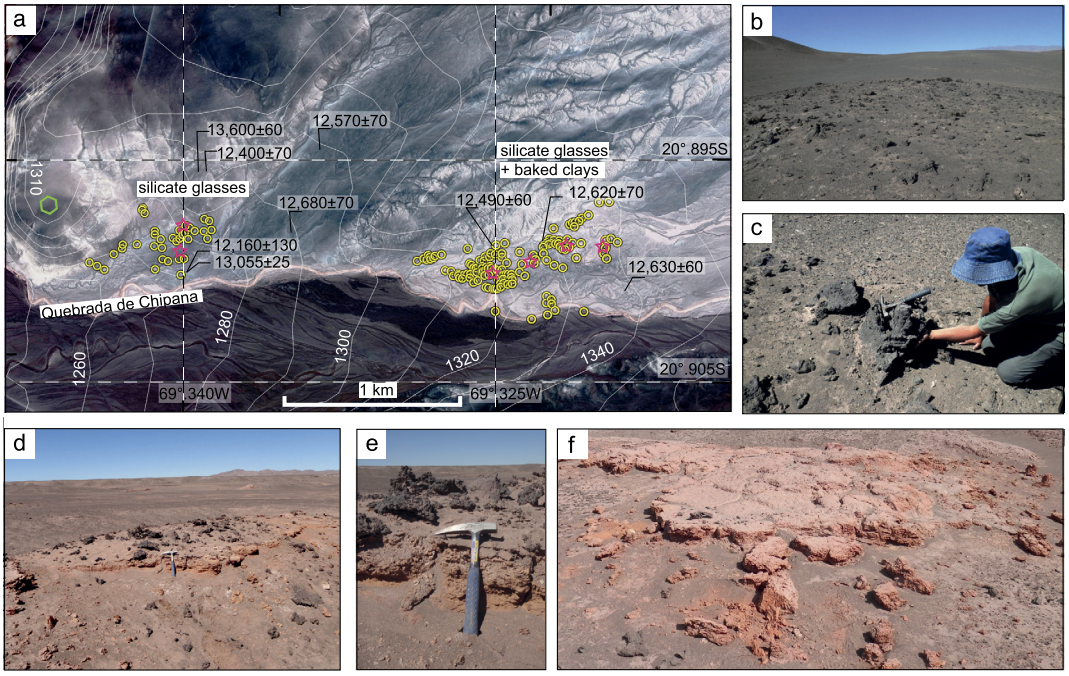

Fig. 3. Field observations at Quebrada de Chipana. (a) Distribution of silicate glasses and baked clays on a satellite image (from Google Earth) with elevation contour line spacing of 10 m. Yellow dots indicate places where glasses and/or baked clays were observed. ^{14}C ages and paleomagnetic sampling (red stars) are shown on the map. Green polygon indicates the flat area with no trace of surface heating, located 50 m above the glass fields. (b, c) Field images of glasses in the westernmost area, (d, e) Silicate glasses overlying a 10 to 20 cm thick layer of red clays, (f) Field image of the layer of baked clays. (For interpretation of the references to color in this figure legend, the reader is referred to the web version of this article.)

Service d'Analyse des Roches et des Minéraux (CRPG) by ICP-OES for the major elements and ICP-MS for the trace elements and REE. Sample preparation, analytical conditions, uncertainty and limits of detection are detailed in Carignan et al. (2001) and in http://helium.crpg.cnrs-nancy.fr/SARM/pages/roches.html. X-ray fluorescence (XRF) analyses for major and trace elements were also

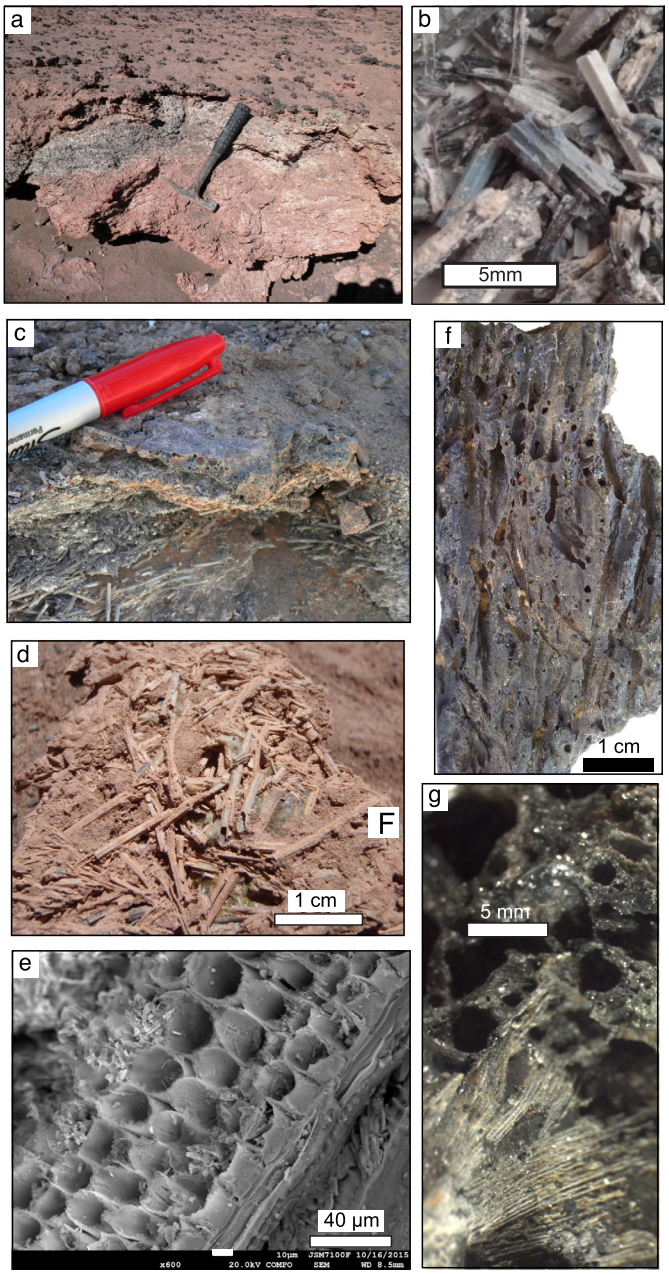

Fig. 4. Plant imprints in Pica glasses. (a) Photograph showing glass overlying a ~20 cm thick layer of silicified plants at Quebrada de Chipana; (b) Silicified wetland plant remains (cf. Cyperaceae); (c) Photograph of a sample of glass overlying a layer of plants (Quebrada de Chipana locality); (d) Silicified twigs within a vitreous matrix; (e) SEM observation of a twig showing the replacement of the plant by silica. (f) Upper surface of a glass sample showing grooves due to plant imprints (Puquio de Nuñez locality); (g) Plant imprint within a glass sample from the NW Pica area.

obtained by the Laboratory of Sernageomin (Chile) in five soil samples from the Puquio area. Platinum-group elements Ir and Pt were measured in only one sample with the Nickel Sulphide Fire assay method and ICP-MS finish at Geosciences Laboratories (Geo Labs, Sudbury, Canada). The elemental composition of the glass was determined by electron microprobe analysis using a Cameca SX-100 at the Centre de Microanalyse de Paris VI (CAMPARIS). To avoid loss of the most volatile elements (Na and Cl in particular), we used a defocused beam of 10 µm diameter, an accelerating voltage of 15 kV, and a beam current of 4 Na. Eleven samples were analyzed, with 3 to 7 glass analyses per sample. The chemical data are reported in Supplementary Dataset S1.

The water content was determined for glassy areas of 1 mm in diameter on ~500 µm thick double-polished sections using FTIR transmission microscopy with a VERTEX V70 spectrometer coupled to a Hyperion 3000 infrared microscope (IPAG Grenoble). Infrared measurement were obtained in the 4000–1000 cm^{-1} spectral range and water contents were estimated by the intensity of the –OH fundamental stretching band at 3550 cm^{-1} (using a molar absorptivity coefficient of 67 L/mol, Stolper, 1982).

3.2. Petrography

The PGs are heterogeneous at the centimeter scale and contain variable amounts of pure glass (10 to 90 vol%, average 50 vol%) (Fig. 5) mixed with relict mineral grains (quartz, feldspars, pyroxenes being the most common), and scarce lithic fragments of volcanic origin. Dendritic crystals of Ca-pyroxene, wollastonite, plagioclase and less frequently melilite that formed during quenching of the glass are also common (Fig. 5d, e), locally associated with skeletal crystals of Ti-poor titanomagnetite. Iron sulphide grains (pyrrhotite or troilite) up to 100 µm are found adjacent to vesicles (Fig. 5b, f, g, and h) but droplets of iron sulphides are also found in the glass (Supplementary Fig. S2). These iron sulphides, especially those within vesicles, often present a weathering pattern typically developed in hot desert climate (Supplementary Fig. S2b). Although the ratio of Fe/S determined by EDS analyses suggests a composition closer to pyrrhotite, their low or undetected magnetic signals suggest that these particles were antiferromagnetic troilite (FeS) grains before weathering. Some samples also contain droplets of Ni-free iron phosphide, generally in association with iron sulphide (Supplementary Fig. S2). EDS analyses indicate a composition close to Fe_3P. Within some glasses, we observed numerous droplets of native iron, iron sulphide, and iron phosphide. All sulphides are Ni-free. Rare metallic iron and iron carbides are also found.

The PGs contains numerous pyroxene crystallites. Relict grains of quartz within the silicate glass do not show evidence of melting. A few titanomagnetite grains show structures suggesting incipient melting and some pyroxene crystals show crystal overgrowth. Pristine zircon grains indicate that the temperature of decomposition of zircon to baddeleyite (~1775 °C, El Goresy, 1965) was never reached.

The PGs exhibit several structures that could be interpreted as flow during melting (Fig. 2a). However, these structures are mostly common in samples that display well organized grooves on the surface and tubes suggesting that the putative flow structure is related to the melting of silicified plants.

3.3. Chemical composition

The bulk compositions of PG are in the range 59–64 wt% SiO_2, 10–15 wt% Al_2O_3, 4–13 wt% Na_2O, 4.7–6.5 wt% CaO, 3–4.5 wt% Fe_2O_3 (Supplementary Dataset S1). At Puquio de Nuñez, the sandy soils (dominated by detrital quartz, plagioclase, K-feldspar, Ca-pyroxene, with accessory zircon, ilmenite, and titanomagnetite) present a slightly more elevated content of SiO_2 (about 66 wt%) relative to the PG. PGs are enriched in either Na_2O or CaO with respect to the sandy soils. PGs are clearly depleted in minor elements, for example in Zr, Pb and Ni, compared to the soils. Sr concentrations are similar in soils and glasses (Supplementary Fig. S3 and Supplementary Dataset S1). Electron microprobe analyses of pure glass from all localities show an average composition similar to that of the whole rock Pica Glass samples (that also contains a significant and variable fraction of unmelted material), but significant inter-sample variations are observed: SiO_2 ranges from 58.5 to 70.7 wt%, and Al_2O_3 from 5.2 to 25.5 wt%, Cl from 0.1 to 2.9 wt%. Bulk siderophile transition element contents are low (Ni $<$ 20 ppm, Co $<$ 12 ppm, Cu $<$ 54 ppm) (Supplementary Fig. S3). The search

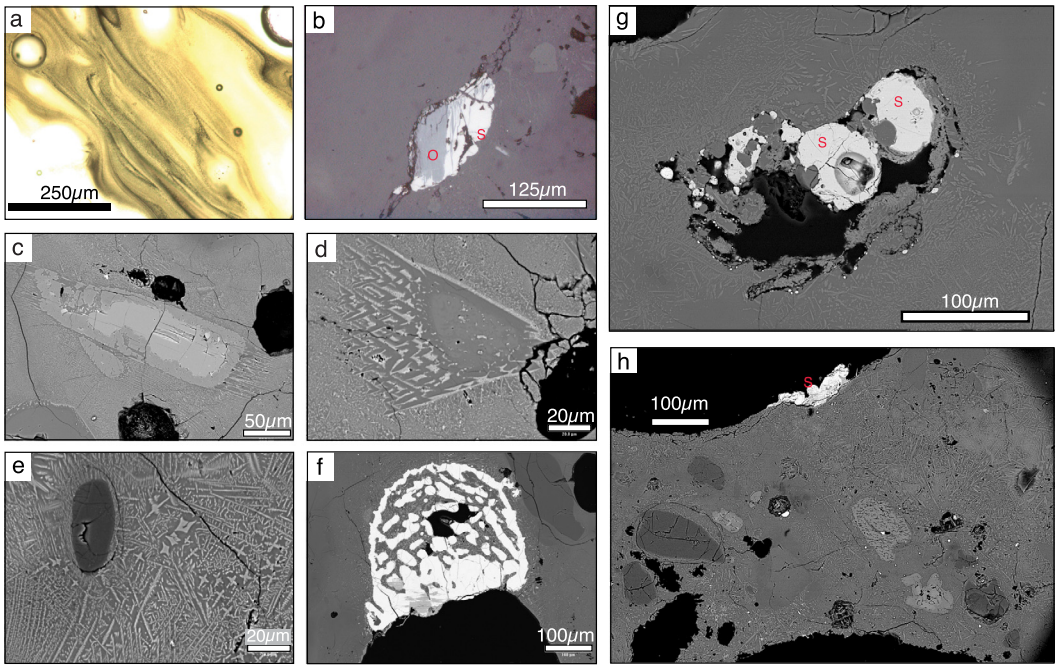

Fig. 5. Microscope observations of Pica glasses. (a) Transmitted light image of a sample with flow-like structure from Puquio de Nuñez. (b) Reflected light image of iron sulphide (S) showing partial weathering-related oxidation (O). (c, d, e) Backscattered Electron (BSE) images of crystallite-rich glass with relict grains and dendritic overgrowths of feldspar and clinopyroxenes, typical of quench textures. (f) Iron sulphide grain nucleated on a vesicle. (g) Large sulphide grains in a vesicle. (h) Detrital grains in a glass matrix.

for highly siderophile element enrichments (platinum-group elements) was unsuccessful (Ir <0.02 ppb; Pt <0.20 ppb). The water content in the glass was determined for 9 samples with 4 to 7 independent measurements by sample. H_2O content is low ($<$ average of 0.298 wt% $\pm$0.197) in all samples, but one shows a large spread with 7 individual measurements ranging from 0.160 wt% to 2.6 wt % (Table S1). The bulk composition of the silicified plants is 50 wt% SiO_2 and CaO 19 wt% (not corrected for the large loss on ignition due to the presence of CO_2 and H_2O) with a notable total S content of 5.2%. SEM observations, however, suggest some late deposition of gypsum and calcium carbonates after the thermal event. The plants are depleted in most minor and trace elements except Sr compared to sands.

4. ^{14}C dating

We obtained ^{14}C ages from 11 samples of charcoal and organic matter from plant remains within the soils containing the PGs (Dataset S2). These ages, and those previously published (Blanco and Tomlinsson, 2013) for the PG-bearing areas (Table 1), correspond to the Pleistocene–Holocene transition (Fig. 6). A similar distribution of ^{14}C ages was also reported (Nester et al., 2007; Gayo et al., 2012) for nearby locations to the south of our study area, and was interpreted as evidence for repeated expansions of riparian/wetland ecosystems, and perennial rivers along the southernmost Pampa del Tamarugal basin from 17.6–14.2 ka, 12.1–11.4 ka and from 1.01–0.71 ka (Gayo et al., 2012) (Supplementary Fig. S4).

All samples from the Puquio de Nuñez area display younger ^{14}C ages than those observed at Quebrada de Chipana (Fig. 6). The two youngest ages were obtained on non-carbonized roots cutting the layer with carbonized plants, thus providing an upper limit for the age of the thermal event. The older ^{14}C ages at Quebrada de Chipana can indicate either that the thermal event at Quebrada de Chipana is significantly older than the one at Puquio de Nuñez or that the ^{14}C ages at Quebrada de Chipana represent ages of organic matter accumulated on the soil surface at least 2000 years prior to the thermal event.

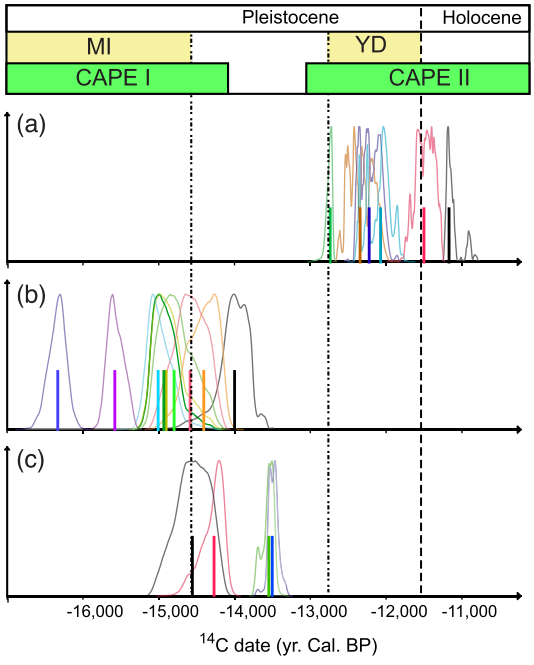

Fig. 6. ^{14}C age determinations. Calibrated ^{14}C age spectra (thick lines for median ages, different colors illustrate different samples, see Table 1). (a) 6 samples from Puquio de Nuñez. (b) 9 samples from Quebrada de Chipana. (c) 2 samples from NW of Pica and Quebrada de Guatacondo. The Mystery Interval (MI) and the Younger Dryas (YD) cold periods at the end of the Pleistocene are highlighted with the yellow boxes while the two phases of Central Andean Pluvial Event (CAPE) (Gayo et al., 2012) are shown in green boxes. (For interpretation of the references to color in this figure legend, the reader is referred to the web version of this article.)

Taking into account the extremely good preservation of organic matter in the Atacama Desert, these ^{14}C ages can only provide a maximum age of the thermal event.

Table 1
^{14}C calibrated ages.

Sample	Sample type	Latitude (°)	Longitude (°)	Age $\pm 1\sigma$	Median calibrated age	
Puquio de Nuñez						
IB-54a[2]	Organic matter in sediment	−20.57839	−69.35879	10,500 ± 70	12,327	[12,044; 12,618]
Ca_PR_A_01[3]	Carbonized organic matter	−20.58253	−69.36117	10,395 ± 50	12,209	[12,001; 12,412]
Ca_PR_A_02[3]	Carbonized organic matter	−20.58275	−69.35937	10,335 ± 50	12,056	[11,824; 12,395]
So_PR_A_02[3]	Soil	−20.58275	−69.35937	10,910 ± 50	12,744	[12,690; 12,828]
Ro_PR_A_02[3]	Plants not carbonized	−20.58275	−69.35937	9760 ± 45	11,156	[10,825; 11,239]
Ro_PR_A_01[3]	Plants not carbonized	−20.58253	−69.36117	10,045 ± 45	11,479	[11,270; 11,708]
Quebrada de Chipana						
IB-101[2]	Organic matter in sediment	−20.89511	−69.33856	13,600 ± 60	16,330	[16,112; 16,580]
N05-21[1]	Organic matter on terrace	−20.90026	−69.34002	13,055 ± 25	15,579	[15,350; 15,756]
IB-102[2]	Organic matter in sediment	−20.89507	−69.33771	12,400 ± 70	14,401	[14,086; 14,803]
N05-22[1]	Organic matter on terrace	−20.90026	−69.34002	12,160 ± 130	13,992	[13,599; 14,481]
IB-105[2]	Shrub vegetation in sediment	−20.89503	−69.33289	12,570 ± 70	14,784	[14,319; 15,116]
Ca_PR_B03[3]	Carbonized organic matter	−20.89863	−69.33481	12,680 ± 70	15,008	[14,669; 15,276]
Pl_PR_B_05[3]	Carbonized plants	−20.89910	−69.32286	12,620 ± 70	14,894	[14,441; 15,192]
Ca_PR_B_H6[3]	Carbonized plant	−20.89917	−69.32536	12,490 ± 60	14,580	[14,210; 14,980]
So_PR_B_G170[3]	Carbonized soil	−20.90114	−69.31972	12,630 ± 60	14,925	[14,538; 15,194]
Quebrada de Guatacondo						
IB-116[2]	Roots remains in sediments	−20.99204	−69.30266	12,470 ± 70	14,540	[14,169; 14,961]
Ca_PR_C_01[3]	Carbonized organic matter	−20.98857	−69.29995	11,700 ± 60	13,487	[13,325; 13,595]
NW of Pica						
IB-138[2]	Roots remains in sediments	−20.44533	−69.41273	12,350 ± 50	14,259	[14,062; 14,634]
Ca_PR_SiteD[3]	Carbonized plants	−20.44747	−69.41294	11,770 ± 60	13,543	[13,443; 13,722]

^{14}C ages [1]From Nester et al. (2007); [2]Blanco et al. (2012); [3]This study. ^{14}C AMS ages (±1 s) determined at the Saclay ^{14}C AMS laboratory (Artemis programme). Additional laboratory information given in Dataset S2 for the ^{14}C ages obtained in this study. Calibration (Cal BP) with the southern hemisphere calibration curve SHcal13.14c (Hogg, 2013) using the Chronomodel software (http://www.chronomodel.fr). Median calibrated age cal yr. BP and confidence interval at 95%.

5. Paleomagnetism

5.1. Paleomagnetic sampling and methods

At Puquio de Nuñez, standard 2.5 cm cores were drilled from unoriented blocks of PG. In blocks with an approximately flat surface, cores were drilled orthogonally to this surface interpreted as paleohorizontal at the time of PG formation. Fifteen glass samples, found in the soil covered by a layer of sand in a position suggesting little or no displacement after emplacement (Fig. 2e), were oriented with a molded horizontal plaster cap.

At Quebrada de Chipana, eight blocks of 10 to 20 cm-thick baked clays and three PG blocks were oriented with a plaster cap. In addition, cores were drilled in 20 PG blocks for which field observations suggested that these were practically *in situ* since the time of formation. The samples were oriented with magnetic and sun compasses. Samples from the baked clays were then consolidated in the laboratory with sodium silicate prior to further subsampling of standard one-inch diameter cores. Up to six cores were drilled in each block. We also took several pieces of unoriented fragments of the fine-grained baked clay beds.

The remanent magnetizations were measured at Géosciences Rennes Laboratory with a 2G SQUID magnetometer and demagnetized thermally in a MMTD furnace or by alternating field (AF) with the 2G online degausser. Thermomagnetic measurements were performed with the Agico susceptibility meter KLY3 equipped with a CS3 furnace. Hysteresis data were obtained on 1 to 3 mg whole rock samples with a Princeton alternating gradient magnetometer at LSCE (Gif/Yvette, France). First order reversal curve (FORC) diagrams were processed with the FORCINEL software (Harrison and Feinberg, 2008).

Determination of the paleointensity of the Earth's magnetic field was attempted on 11 of the baked clay samples and on 85 PG samples using the original Thellier and Thellier (Thellier and Thellier, 1959; Chauvin et al., 2005) or the IZZI (Tauxe and Staudigel, 2004) procedure. For thermoremanent magnetization (TRM) acquisition, the samples were heated and cooled in air or in vacuum ($<10^{-2}$ mbar) under an applied dc field (Dataset S3) ranging from 30 to 50 μT. Experiments were performed either on whole cores or on small fragments of unoriented samples that were fixed in a quartz tube using non-magnetic glass fibers and sodium silicate. A partial TRM check was performed every two temperature steps to check for heating induced mineralogical changes.

Archeomagnetic studies on bricks and ceramics have often shown a strong anisotropy of TRM. Thus, the magnetic anisotropy of the baked clays was determined with TRM acquisition in six positions ($+x, -x, +y, -y, +z, -z$). The cooling rate effect (Yu, 2011) on paleointensity determinations was tested only on the baked clays using a constant cooling rate of 0.3 °C/mn compared to the fastest cooling rate (>10 °C/mn) used for the routine paleointensity experiments.

5.2. Magnetic properties

Baked clay samples (Quebrada de Chipana) have the highest magnetic susceptibility and natural remanent magnetization (NRM) while the magnetic properties of the glasses at Puquio de Nuñez differ clearly from those at Quebrada de Chipana (Fig. 7).

PG samples with a large amount of glass at Puquio de Nuñez have the lowest NRM. The highest magnetic content of PG samples at Quebrada de Chipana is related to the highest content in relict grains and magnetite crystallites in the glass matrix. Samples from Quebrada de Guatacondo have a wide range of magnetic properties overlapping those of the Puquio de Nuñez and Quebrada de Chipana fields.

All samples of baked clays and silicate glasses record stable univectorial characteristic remanent magnetizations (ChRMs). Silicate glasses have a high stability upon AF demagnetization with high median destructive fields, allowing us to dismiss a possible lightning effect (Fig. 7).

The baked clays have two magnetic phases: magnetite, and a higher coercivity phase carrying from 10 to 60% of the remanent magnetization not demagnetized above 100 mT (Fig. 7). The two phases are also recognized in hysteresis data (Fig. S5). This be-

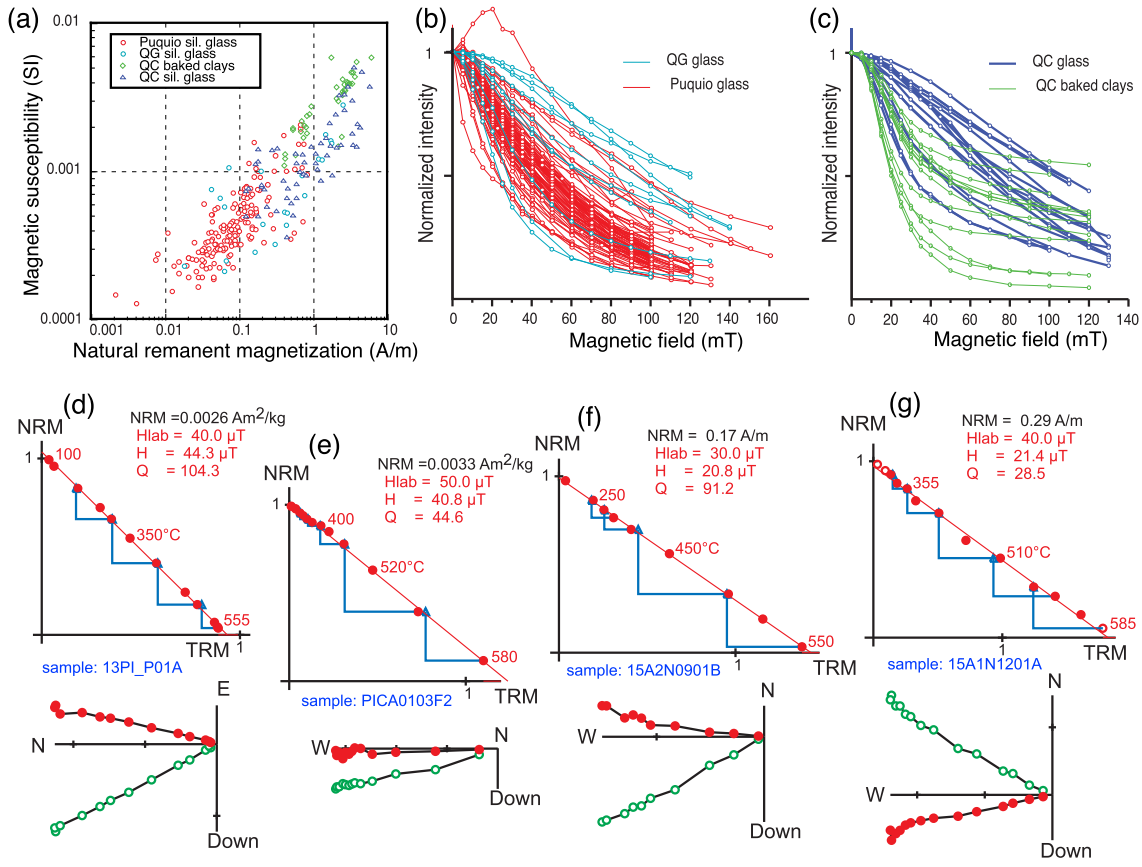

Fig. 7. Magnetic properties and representative paleointensity results. (a) Magnetic susceptibility versus the intensity of the NRM showing significant variations of magnetic properties between the glasses at Puquio de Nuñez and Quebrada de Chipana (QC), and within the Quebrada de Guatacondo (QG) glass field; (b, c) Variation of the intensity of the NRM during alternating field demagnetization for silicate glasses and baked clays; Paleointensity diagrams and associated orthogonal plots for a sample of baked clay (d), silicate glasses at Quebrada de Chipana (e) and Puquio de Nuñez (f and g). Red filled symbols correspond to points used to determine the slope of the best-fit line in the NRM-TRM plot. Triangles correspond to PTRM checks. For orthogonal plots, open green (filled red) symbols are projection in the vertical and horizontal plane, respectively. (For interpretation of the references to color in this figure legend, the reader is referred to the web version of this article.)

havior is often observed in archeomagnetic studies on bricks. The high coercivity phase is common in bricks fired at high temperatures, and is likely due to the transformation of iron-rich clays at high temperatures. Distributed unblocking temperatures in the range 200–550 °C is also a characteristic of archeomagnetic materials (Chauvin et al., 2000; McIntosh et al., 2011). We can conclude, therefore, that the baked soils in the present study have likely reached temperatures similar to those used to form archeological bricks (~700 °C or above).

All glass samples show hysteresis cycles characteristic of magnetite, except one with saturation above 0.5 T indicating a possible contribution from metallic iron (Supplementary Fig. S5). No evidence of pyrrhotite was found in thermomagnetic experiments. Further work is needed to decipher the possible contribution of iron sulphides to the magnetic signal.

5.3. Paleomagnetic directions

The baked clays at Quebrada de Chipana record well-clustered ChRM directions (Fig. 8), except for one sample probably taken on a more disrupted part of the baked clay.

The direction of the PG at Quebrada de Chipana present some scatter because the blocks have likely been slightly disturbed since their formation but the mean ChRM direction determined from the glasses is indistinguishable from the one recorded by the baked clays (Table 2, Fig. 8).

ChRMs were determined for fifteen oriented samples at Puquio de Nuñez. The mean paleomagnetic direction recorded by the PG at Puquio de Nuñez is statistically different from the mean direction recorded by the baked clays or the PG at Quebrada de Chipana (Fig. 8). In order to further constrain the paleomagnetic test, we also determined the ChRM directions obtained from cores drilled perpendicular to nearly flat PG surface in 61 non-oriented blocks found lying at the surface. Nine samples have a positive inclination at more than 45° from the mean direction. The mean inclination (angle to the surface) determined from the other 52 unoriented blocks is −21.8° with an angle of confidence at 95% of 7.2° (Table 2). The nine samples yielding high positive inclinations were interpreted as overturned samples. If we invert the inclination for these samples, the mean inclination for the 61 samples is −24.8° ± 6.7°. This mean inclination determined in the unoriented PG samples is in agreement with the inclination recorded by the oriented PG blocks.

At Quebrada de Guatacondo, the number of oriented cores is too low for a statistical comparison with the paleomagnetic result in the baked clays at Quebrada de Chipana.

5.4. Paleointensity experiments

Paleointensity determinations were attempted on 96 samples. 70 samples provided results with acceptable quality (Fig. 7, Supplementary Fig. S6, Dataset S3). This high success rate is due to a NRM carried mainly by single domain grains of magnetite. The quality factor q is greater than 29 for more than 50% of the samples. PG samples with optical evidence of iron sulphides in the vesicles were the most affected by alteration during heating. This

Table 2
Paleomagnetic results.

a) Characteristic directions					
Localities	n/N	Dec (°)	Inc (°)	k	$\alpha 95$
QC baked clays	7/8	351.6	−40.5	373	3.1
QC glass	22/23	345.7	−40.7	16	8.0
PN glass	14/15	9.4	−18.6	31	7.2
PN glass[1]	52/61		−21.8	8.4	7.2
PN glass[2]	61/61		−24.8	8.5	6.7
QG glass	5/5	2.3	−35.0	57	10.2

b) Paleointensity results				
	N	Field (μT)	VDM (10^{22} Am^2)	VADM (10^{22} Am^2)
QC baked clays	11	41.2 ± 3.5	8.8	9.1
QC baked clays[3]	11	41.8 ± 2.7	8.9	9.2
QC baked clays[4]	11	39.4 ± 1.7	8.4	8.7
QC glass	18	39.7 ± 3.5	8.5	8.7
PN glass[5]	26	20.9 ± 1.2	5.0	4.6
PN glass[6]	10	38.1 ± 3.0		8.4
PN glass	36	25.7 ± 7.9		5.7
QG glass	5	39.8 ± 4.6	8.9	8.8

a) Mean-site ChRM directions. n/N, number of samples included in the mean calculation versus number of studied samples; Dec, Inc, mean declination and inclination; k, Fisher concentration parameter; $\alpha 95$ semi-angle of confidence at 95%. [1] Mean inclination determined from vertical cores after rejection of 9 samples with positive inclinations at more than 45° from the mean, [2] Positive inclinations inverted for nine samples assuming that the positive inclination may correspond to overturned blocks. b) Paleointensity results, N, number of samples; Field, weighted paleointensity mean value and standard deviation; VDM, VADM, Virtual dipole moment and Virtual axial dipole moment, respectively. For baked clays, after anisotropy [3] and cooling rate corrections [4]; Paleointensity data from Puquio de Nuñez fall in two distinct groups, mean for the group with low [5] or high [6] paleointensity data. PN, Puquio de Nuñez, QC, Quebrada de Chipana, QG, Quebrada de Guatacondo.

was easily characterized by the acquisition of a Chemical Remanent Magnetization in the direction of the applied field during the first step of the paleointensity experiment above ∼300 °C (Supplementary Fig. S6).

The baked clays provide very high-quality paleointensity results with q up to 150. The magnetic anisotropy correction is low. A laboratory cooling rate overestimate effect of 5 to 7% was observed in all samples except sample 13PI_P10a. These results are typical of those observed in archeological studies on bricks (Chauvin et al., 2000). It is difficult to estimate the natural cooling rate but cooling below 200°C is likely to occur within hours taking into account the thickness of the baked layer (20-40 cm). Thus the initial cooling rate is likely near the slowest cooling rate used in the laboratory supporting the application of the laboratory cooling rate correction.

The baked clays at Quebrada de Chipana give a well-defined paleointensity of 39.4 ± 1.6 μT after correction for anisotropy and cooling rate. The mean value from 18 determinations on PG samples from the Quebrada de Chipana locality is similar to the mean paleointensity determined for the baked clays (Fig. 8, Table 2).

The determination of the paleointensity was successful in 36 specimens at Puquio de Nuñez and most samples from the Puquio de Nuñez area provide significantly lower paleointensities than those observed in the baked clay samples of Quebrada de Chipana (Fig. 8). Two groups of paleointensity values are observed. Twenty six determinations from 25 independent PG blocks provide a low field value of 20.9 ± 1.2 μT. The other group of 10 determinations, but from only three different blocks, provides a mean paleointensity value similar to the one at Quebrada de Chipana and at Quebrada de Guatacondo (Table 2).

The paleomagnetic directions and the paleointensity results are statistically different at Puquio de Nuñez and Quebrada de Chipana which are separated only by a few tens of km. This observation demonstrates that the thermal events at Puquio de Nuñez and Quebrada de Chipana did not occur under the same geomagnetic field configuration. The differences between the ChRM directions (∼20°) and paleointensity results (∼20 μT) at Puquio de Nuñez and Quebrada de Chipana are large enough to indicate the record of a significant secular variation of the Earth's magnetic field. Such variations in inclination and intensity are only reasonable over a few centuries. For instance, such variations have occurred in Chile over the last three centuries (Roperch et al., 2015) that are characterized by very high rate of variations in magnetic inclination (up to 0.12°/yr) and in field intensity (up to 0.15 μT/yr). Altogether, the paleomagnetic data prove that the glasses at Quebrada de Chipana and Puquio de Nuñez have ages differing by at least a few hundred years.

5.5. Paleomagnetic test of a thermal event away from the glass fields

If the Pica glasses were formed during an airburst, evidence of heating at high temperature should also be found immediately outside the glass fields. About 200 m north of the Quebrada de Chipana, at an elevation about 50 m above the glass field, there is a meseta without glasses but with clasts of silicified limestone lying at the surface (Fig. 3a). In view of the extremely low erosion rates and surface stability in the Atacama Desert since the Miocene (Dunai et al., 2005), these clasts were likely already on the surface at the time of the formation of the Pica glasses. We collected 15 unoriented clasts with sizes around 5 cm to test the hypothesis of a partial thermal remagnetization event. The samples were demagnetized in zero field and remagnetized in a field of 40 μT as in the paleointensity experiments. The TRM acquired in the laboratory at 460 °C are up to 10 times the intensity of the NRM. There is no

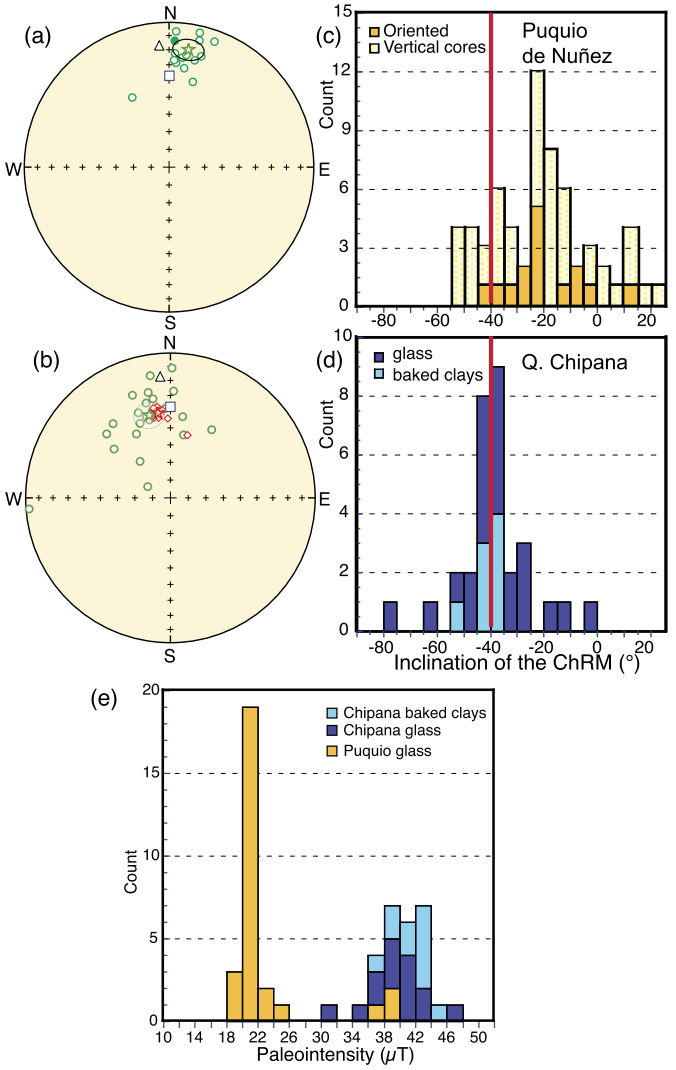

Fig. 8. (a) Equal-area projections of the paleomagnetic directions determined in oriented samples at Puquio de Nuñez (open, filled symbols for respectively negative, positive inclinations. (b) Paleomagnetic directions at Quebrada de Chipana (glasses shown in green circles; baked clays with red diamonds). (c, d) Paleomagnetic inclinations at Puquio de Nuñez and Quebrada de Chipana. (e) Geomagnetic paleointensities determined in samples from Puquio de Nuñez and Quebrada de Chipana. (For interpretation of the references to color in this figure legend, the reader is referred to the web version of this article.)

paleomagnetic evidence for any significant thermal event having affected the clasts. Moreover, most samples showed profound color changes during heating above 400 °C, indicating that they were not heated above this temperature since their formation. Overall, these experiments indicate that this surface, located only 200 m away from the glass fields, was never heated significantly.

6. Discussion

The areal extent of the Pica Glass and their composition are unlike any known historical or prehistoric metallurgy slag deposit, precluding an anthropogenic origin. The location (70 km west of the closest volcanic arc), the shape and size of the blocks, and the mineralogy are inconsistent with a volcanic origin.

Glassy rocks, called fulgurites, can be formed in the subsoil by lightning in the form of hollow tubes (Sponholz et al., 1993; Pasek et al., 2012). They are usually 1–2 cm in diameter, with millimeter thick walls, but can reach several meters depth and diameters of up to 15 cm in exceptional circumstances. These characteristics strongly contrast with the observed extended areal distribution of the PG and with the occurrence of baked soils over an area of 0.1 km^2. Heating of this thick baked layer or the formation of glasses by lightning would imply an unrealistic number of lightning strikes on the same surface. Moreover none of the PG and associated baked clay samples shows remagnetization by strong fields (Fig. 7), which would be expected in case of successive adjacent lightning strikes.

Another possible formation mechanism for surface glasses is hypervelocity impact (French and Koeberl, 2010). The Pica glasses cannot be distal impact ejecta deposits because such ejecta could not produce a 20 cm-thick layer of baked clays. We found no geochemical evidence for contamination by an impacting body, with no enrichment in metallic or platinoid elements in the glass. Textural evidence shows that iron sulphide droplets were formed *in situ* mostly on the walls of gas vesicles (Fig. 5, Fig. S2).

The large spread of ^{14}C ages and the different paleomagnetic fields (direction and intensity) between localities Puquio de Nuñez and Quebrada de Chipana show that the glasses were not formed synchronously at these sites, and thus cannot have formed during a single thermal event triggered by a large airburst. Just as important is the lack of surface thermal event on the mesas immediately adjacent to the specific low-elevation areas where glasses are found at Quebrada de Chipana.

The only remaining viable hypothesis to account for the formation of the Pica glasses is akin to pyrometamorphism during coal fires (Grapes, 2011; Stracher et al., 2011) or methane flares forming paralavas (Grapes et al., 2013). The grooves on the surface of PG blocks and tube-shape cavities found in many samples are remnants of melted silicified plants and twigs. These plant remnants and imprints indicate that vegetation played a pivotal role in the formation of the glasses. Cases of glass formation during fires of phytolith-rich plants have been reported (Vélain, 1878; Baker and Baker, 1963). Vélain (1878) made the first petrographic description of glasses found within ashes after haystack fires in France. He clearly related the chemical composition of the glasses to the nature and type of the burned hay or wheat, and pointed out that the extraterrestrial origin, popularly attributed to these unusual glasses in the 19th century, was only the result of superstition. Baker and Baker (1963) also made a detailed description of silica glass formation during the burning of two large haystacks in Australia. Fusion and melting of the opal phytoliths contained in the ~325 tons of pasture plants yielded about 16 tons of silica glass (Baker and Baker, 1963).

The ^{14}C ages of the plant remains further correlate with the timing of the two phases of the Central Andean Pluvial Event (CAPE) (Fig. S5), a multi-millennial scale event of increased rainfall in the high Andes (Quade et al., 2008), which are roughly coeval with the two major periods of sea surface temperature drops in the north Atlantic (the so-called Mystery Interval and the Younger Dryas) (Broecker et al., 2010). These two periods also correspond for the most part to the maximum highstands of paleolake Tauca nearly 100 m above the present-day surface of the salar de Uyuni and salar de Coipasa that cover a large area of the southern Bolivian Altiplano (Fig. 1) (Sylvestre et al., 1999; Plackzek et al., 2006; Blard et al., 2009; Gayo et al., 2012; Quesada et al., 2015). As precipitation in the high Andes increased discharge and elevated groundwater tables (Quade et al., 2008), large oases formed throughout the western Andean piedmont across the Atacama Desert (Rech et al., 2002, 2003; Saez et al., 2016). The present-day distribution of the glasses at Puquio de Nuñez roughly corresponds to a paleowetland extending more than 3 km to the north of the present-day Puquio de Nuñez small oasis. Except for brief interludes of increased groundwater tables (2.5–1.7 ka, and 1.01–0.71 ka) most of the Holocene has been hyperarid in the Atacama (Gayo et al., 2012).

We thus propose that the Pica glasses were produced *in situ* by fires in dry wetland soils rich in organic matter and siliceous plant remains (Pigati et al., 2014). Microscopic observations in thin section of apparent flow structures in samples displaying surface grooves suggest that the structures are likely remnants of melted elongated silicified plants. The water content in the glass is low (average of 0.298 wt% ±0.197, Table S1), but above the range for most impact glasses (Beran and Koeberl, 1997). Beran and Koeberl (1997) suggest that only very low H_2O contents in glasses (<0.05 wt%) are diagnostic of an origin by impact. Microprobe analyses indicate high Cl values (up to 2.87 wt%) which have also been observed in paralavas (Grapes et al., 2013). In some samples, the silicified remains were not always fully melted during burning of the organic matter.

The Pica glasses contain detrital relict grains within the glass and the whole-rock chemical composition of such glasses is intermediate between those of the desert sandy soil and the silicified plants. Soils with abundant organic matter and SiO_2-rich phytoliths, clay minerals and salts (sodium chloride, sodium and calcium sulfates, carbonates, possible nitrates) may have melted at lower temperatures than needed to melt detrital quartz grains.

Temperatures reached during natural fires are usually low at the soil surface (Stoof et al., 2013) but may rapidly increase in cases of underground burning inside an organic matter-rich layer beneath a sand lid as in the case of smoldering combustion during peat fires (Rein et al., 2008). Very few examples of natural subsurface combustion leading to soil fusion have been reported. Monod and Palausi (1961) first reported evidence of melted rocks near Lake Faguibine (Mali) but this observation was later mistakenly interpreted as incipient volcanism (El Abbass et al., 1993). However, Svensen et al. (2003) demonstrated that subsurface combustion is the source of heat and the cause for soil melting. These authors suggest that the surface combustion in the Timbuktu region today could be a common phenomenon in northern West Africa. Our observations in the Atacama Desert suggest that such fires, especially when very dry conditions facilitated the propagation of the smoldering front (Prat-Guitart et al., 2016), may account for the formation of similar irregular slag-like glassy rocks previously attributed to melting of surface sediments during airbursts (Haines et al., 2001; Schultz et al., 2004; Osinski et al., 2008). Indeed, the airburst hypothesis for the formation of surface glass mainly relies on numerical simulations (Wasson, 2003; Shuvalov and Trubetskaya, 2007; Boslough and Crawford, 2008). As an example, the Dakhleh glass has been attributed to an airburst (Osinski et al., 2008, 2007), but evidence for this is sketchy (Reimold and Koeberl, 2014). It is noteworthy that the Dakhleh glass shares numerous characteristics with the PG. In particular they are confined around oases and show abundant plant imprints. The similar paleoenvironment at Pica and Dakhleh suggests that specific paleogeographic conditions may be necessary to form this type of glasses. The interpretation proposed for the Pica glass may apply to the Dakhleh glass as well. Similarly, several glass levels with morphological biosignatures such as phytoliths have been reported in the Argentine Pampa (Schultz et al., 2014) and interpreted as evidence for seven successive local asteroid airburst events since the late Miocene, with implications for the occurrence rate of such catastrophic events. We suggest that these glasses may instead have also formed by successive *in situ* fires.

We propose that melting of soils and silica-rich plants during the burning of organic matter-rich layers does not require an external event like an airburst but can be caused by natural fires under specific paleoenvironmental conditions, such as strong climatic oscillations in arid regions. Self-ignition due to exothermal microbial decomposition has been proposed for other examples of peat-fires (Chateauneuf et al., 1986; Svensen et al., 2003) but humans could also have triggered these fires, and a late Pleistocene archaeological site (ca. 13–11 ka) is also known in the area (Latorre et al., 2013).

The two distinct periods of formation of the Pica glasses refute any link with a single global worldwide catastrophic impact event, such as the one suggested to have triggered climate change at the onset of the Younger Dryas (Firestone et al., 2007; Bunch et al., 2012; and Wittke et al., 2013), a theory that is strongly debated (e.g., Pigati et al., 2012; Boslough et al., 2013; Holliday et al., 2014; Meltzer et al., 2014; Van Hoesel et al., 2014). The complex mineralogical assemblage found in the Pica glasses further demonstrates that the presence of iron sulphides, spherules of magnetite, iron droplets or iron phosphides do not necessarily indicate an hypervelocity impact event, as fire in a subsurface layer rich in organic matter may result in the formation of such exotic minerals by reduction of sulfates and iron oxides.

7. Conclusions

^{14}C dating and paleomagnetism demonstrate that the studied silicate surface glasses from the Atacama Desert were formed at the end of the Pleistocene during two or more thermal events separated by at least several hundred years.

The glasses are distributed across the surface of paleowetland deposits. They were formed by melting of partially silicified plants and/or phytoliths-rich soils. Extensive wetlands developed in the Atacama Desert during the latest Pleistocene due to an elevated groundwater table associated with the Central Andean Pluvial Event (an multi-millennial wet event roughly coeval with the Mystery interval and Younger Dryas) and the maximum highstands of paleolake Tauca in the Bolivian Altiplano. Organic matter from grasses and sedges accumulated in soils during these wet periods. Subsequent dry periods triggered fires and smoldering combustion in the soil and plant litter with a very low moisture content. The strong climate oscillations during the Late Pleistocene would have provided such conditions for near-surface vitrification by fire.

Our results provide clues for revisiting other documented cases of unusual silicate glasses that have been previously attributed to airbursts generated by the entry of large meteoroids in the Earth's atmosphere, with implications for the determination of the rate of occurrence of such events on Earth (Boslough and Crawford, 2008), and the possible preservation of fossil life in impact glasses on planetary surfaces (Schultz et al., 2014).

Acknowledgements

We thank N. Blanco and A. Tomlinson for sharing information about the location of the Pica glasses and discussions about their origin. We thank F. Gouttefangeas and L. Joanny for their help in SEM data acquisition and S. Perroud and K. Narea for their help in the field. Discussions with M. Jolivet about paralavas, with D. Marguerie and P. Pengrech about melting conditions were very useful. This study was funded by the Programme National de Planétologie (INSU/CNES), Artemis projects (INSU,CNRS), OSU Rennes and Fondecyt project N° 3140562. C.L. also acknowledges ongoing support from the IEB (grant PFB-23) and Anillo SOC 1405. We thank Dr. Wolf Uwe Reimold and an anonymous reviewer for their help in the elaboration of the final manuscript.

Appendix A. Supplementary material

Supplementary material related to this article can be found online at http://dx.doi.org/10.1016/j.epsl.2017.04.009. These data include the Google map of the most important areas described in this article.

References

Baker, G., Baker, A.A., 1963. Hay–silica glass from Gnarkeet, Western Victoria. Mem. Natl. Mus. Vic., 21–35.

Barrat, J.A., Jahn, B.M., Amossé, J., Rocchia, R., Keller, F., Poupeau, G.R., Diemer, E., 1997. Geochemistry and origin of Libyan Desert glasses. Geochim. Cosmochim. Acta 61, 1953–1959. http://dx.doi.org/10.1016/S0016-7037(97)00063-X.

Beran, A., Koeberl, C., 1997. Water in tektites and impact glasses by Fourier-transformed infrared spectrometry. Meteorit. Planet. Sci. 32, 211–216. http://dx.doi.org/10.1111/j.1945-5100.1997.tb01260.x.

Blanco, N., Tomlinsson, A.J., 2013. Carta Guatacondo. Región de Tarapacá. Carta Geológica de Chile.

Blanco, N., Vásquez, P., Sepúlveda, F., Tomlinsson, A.J., Quezada, A., Ladino, U.M., 2012. Levantamiento Geológico para el Fomento de la Exploración de Recursos Minerales e Hídricos de la Cordillera de la Costa, Depresión Central Y Precordillera de la Región de Tarapacá (20°–21°S). Informe registrado No. IR-12-50. Subdirección Nacional de Geología. Servicio Nacional de Geología y Minería de Chile.

Blard, P.-H., Lavé, J., Farley, K.A., Fornari, M., Jiménez, N., Ramirez, V., 2009. Late local glacial maximum in the Central Altiplano triggered by cold and locally-wet conditions during the paleolake Tauca episode (17–15 ka, Heinrich 1). Quat. Sci. Rev. 28, 3414–3427. http://dx.doi.org/10.1016/j.quascirev.2009.09.025.

Boslough, M.B.E., Crawford, D.A., 2008. Low-altitude airbursts and the impact threat. Int. J. Impact Eng. 35, 1441–1448. http://dx.doi.org/10.1016/j.ijimpeng.2008.07.053.

Boslough, M., Nicoll, K., Holliday, V., Daulton, T.L., Meltzer, D., Pinter, N., Scott, A.C., Surovell, T., Claeys, P., Gill, J., Paquay, F., Marlon, J., Bartlein, P., Whitlock, C., Grayson, D., Jull, A.J.T., 2013. Arguments and evidence against a Younger Dryas impact event. In: Giosan, L., Fuller, D.Q., Nicoll, K., Flad, R.K., Clift, P.D. (Eds.), Geophysical Monograph Series. American Geophysical Union, Washington, D. C., pp. 13–26.

Broecker, W.S., Denton, G.H., Edwards, R.L., Cheng, H., Alley, R.B., Putnam, A.E., 2010. Putting the Younger Dryas cold event into context. Quat. Sci. Rev. 29, 1078–1081. http://dx.doi.org/10.1016/j.quascirev.2010.02.019.

Brown, P.G., Assink, J.D., Astiz, L., Blaauw, R., Boslough, M.B., Borovicka, J., Brachet, N., Brown, D., Campbell-Brown, M., Ceranna, L., Cooke, W., de Groot-Hedlin, C., Drob, D.P., Edwards, W., Evers, L.G., Garces, M., Gill, J., Hedlin, M., Kingery, A., Laske, G., Le Pichon, A., Mialle, P., Moser, D.E., Saffer, A., Silber, E., Smets, P., Spalding, R.E., Spurny, P., Tagliaferri, E., Uren, D., Weryk, R.J., Whitaker, R., Krzeminski, Z., 2013. A 500-kiloton airburst over Chelyabinsk and an enhanced hazard from small impactors. Nature 503, 238–241.

Bunch, T.E., Hermes, R.E., Moore, A.M.T., Kennett, D.J., Weaver, J.C., Wittke, J.H., DeCarli, P.S., Bischoff, J.L., Hillman, G.C., Howard, G.A., Kimbel, D.R., Kletetschka, G., Lipo, C.P., Sakai, S., Revay, Z., West, A., Firestone, R.B., Kennett, J.P., 2012. Very high-temperature impact melt products as evidence for cosmic airbursts and impacts 12,900 years ago. Proc. Natl. Acad. Sci. 109, E1903–E1912. http://dx.doi.org/10.1073/pnas.1204453109.

Carignan, J., Hild, P., Mevelle, G., Morel, J., Yeghicheyan, D., 2001. Routine analyses of trace elements in geological samples using flow geostand injection and low pressure on-line liquid chromatography coupled to ICP-MS: a study of geochemical reference materials BR, DR-N, UB-N, AN-G and GH. Geoanal. Res. 25, 187–198. http://dx.doi.org/10.1111/j.1751-908X.2001.tb00595.x.

Chateauneuf, J.-J., Faure, H., Lezine, A.-M., 1986. Facteurs contrôlants la génèse et la destruction des tourbes tropicales du littoral Ouest-Africain. Doc. Bur. Rech. Géol. Min. 110, 77–91.

Chauvin, A., Garcia, Y., Lanos, P., Laubenheimer, F., 2000. Paleointensity of the geomagnetic field recovered on archaeomagnetic sites from France. Phys. Earth Planet. Inter. 120, 111–136. http://dx.doi.org/10.1016/S0031-9201(00)00148-5.

Chauvin, A., Roperch, P., Levi, S., 2005. Reliability of geomagnetic paleointensity data: the effects of the NRM fraction and concave-up behavior on paleointensity determinations by the Thellier method. Phys. Earth Planet. Inter. 150, 265–286. http://dx.doi.org/10.1016/j.pepi.2004.11.008.

Dunai, T.J., González López, G.A., Juez-Larré, J., 2005. Oligocene–Miocene age of aridity in the Atacama Desert revealed by exposure dating of erosion-sensitive landforms. Geology 33, 321. http://dx.doi.org/10.1130/G21184.1.

El Goresy, A., 1965. Baddeleyite and its significance in impact glasses. J. Geophys. Res. 70, 3453–3456. http://dx.doi.org/10.1029/JZ070i014p03453.

El Abbass, T., Person, A., Gérard, M., Albouy, Y., Sauvage, M., Sauvage, J.-F., Bertil, D., 1993. Arguments géophysiques et géologiques en faveur de manifestations volcaniques récentes dans la région du lac Faguibine (Mali). C. R. Acad. Sci. Paris, Sér. II 316, 1303–1310.

Firestone, R.B., West, A., Kennett, J.P., Becker, L., Bunch, T.E., Revay, Z.S., Schultz, P.H., Belgya, T., Kennett, D.J., Erlandson, J.M., Dickenson, O.J., Goodyear, A.C., Harris, R.S., Howard, G.A., Kloosterman, J.B., Lechler, P., Mayewski, P.A., Montgomery, J., Poreda, R., Darrah, T., Hee, S.S.Q., Smith, A.R., Stich, A., Topping, W., Wittke, J.H., Wolbach, W.S., 2007. Evidence for an extraterrestrial impact 12,900 years ago that contributed to the megafaunal extinctions and the Younger Dryas cooling. Proc. Natl. Acad. Sci. 104, 16016–16021. http://dx.doi.org/10.1073/pnas.0706977104.

French, B.M., Koeberl, C., 2010. The convincing identification of terrestrial meteorite impact structures: what works, what doesn't, and why. Earth-Sci. Rev. 98, 123–170. http://dx.doi.org/10.1016/j.earscirev.2009.10.009.

Gayo, E.M., Latorre, C., Jordan, T.E., Nester, P.L., Estay, S.A., Ojeda, K.F., Santoro, C.M., 2012. Late Quaternary hydrological and ecological changes in the hyperarid core of the northern Atacama Desert (∼21°S). Earth-Sci. Rev. 113, 120–140. http://dx.doi.org/10.1016/j.earscirev.2012.04.003.

Graham, K.W.T., 1961. The re-magnetization of a surface outcrop by lightning currents. Geophys. J. Int. 6, 85–102. http://dx.doi.org/10.1111/j.1365-246X.1961.tb02963.x.

Grapes, R.H., 2011. Pyrometamorphism, 2nd ed. Springer-Verlag, Berlin, New York.

Grapes, R., Sokol, E., Kokh, S., Kozmenko, O., Fishman, I., 2013. Petrogenesis of Na-rich paralava formed by methane flares associated with mud volcanism, Altyn-Emel National Park. Kaz. Contrib. Miner. Petrol. 165, 781–803. http://dx.doi.org/10.1007/s00410-012-0835-4.

Haines, P.W., Jenkins, R.J.F., Kelley, S.P., 2001. Pleistocene glass in the Australian desert: the case for an impact origin. Geology 29, 899. http://dx.doi.org/10.1130/0091-7613(2001)029<0899:PGITAD>2.0.CO;2.

Harrison, R.J., Feinberg, J.M., 2008. FORCinel: an improved algorithm for calculating first-order reversal curve distributions using locally weighted regression smoothing. Geochem. Geophys. Geosyst. 9. http://dx.doi.org/10.1029/2008GC001987.

Hogg, A., 2013. SHCal13 Southern Hemisphere calibration, 0–50,000 years cal BP. Radiocarbon 55, 1889–1903. http://dx.doi.org/10.2458/azu_js_rc.55.16783.

Holliday, V.T., Surovell, T., Meltzer, D.J., Grayson, D.K., Boslough, M., 2014. The Younger Dryas impact hypothesis: a cosmic catastrophe. J. Quat. Sci. 29, 515–530. http://dx.doi.org/10.1002/jqs.2724.

Kramers, J.D., Andreoli, M.A.G., Atanasova, M., Belyanin, G.A., Block, D.L., Franklyn, C., Harris, C., Lekgoathi, M., Montross, C.S., Ntsoane, T., Pischedda, V., Segonyane, P., Viljoen, K.S. (Fanus), Westraadt, J.E., 2013. Unique chemistry of a diamond-bearing pebble from the Libyan Desert Glass strewnfield, SW Egypt: evidence for a shocked comet fragment. Earth Planet. Sci. Lett. 382, 21–31. http://dx.doi.org/10.1016/j.epsl.2013.09.003.

Latorre, C., Santoro, C.M., Ugalde, P.C., Gayo, E.M., Osorio, D., Salas-Egaña, C., De Pol-Holz, R., Joly, D., Rech, J.A., 2013. Late Pleistocene human occupation of the hyperarid core in the Atacama Desert, Northern Chile. Quat. Sci. Rev. 77, 19–30. http://dx.doi.org/10.1016/j.quascirev.2013.06.008.

McIntosh, G., Kovacheva, M., Catanzariti, G., Donadini, F., Lopez, M.L.O., 2011. High coercivity remanence in baked clay materials used in archeomagnetism. Geochem. Geophys. Geosyst. 12, Q02003. http://dx.doi.org/10.1029/2010GC003310.

Meltzer, D.J., Holliday, V.T., Cannon, M.D., Miller, D.S., 2014. Chronological evidence fails to support claim of an isochronous widespread layer of cosmic impact indicators dated to 12,800 years ago. Proc. Natl. Acad. Sci. 111, E2162–E2171. http://dx.doi.org/10.1073/pnas.1401150111.

Monod, T., Palausi, G., 1961. Sur des manifestations fissurales de laves à néphéline au sud du lac Faguibine (Mali). Bull. IFAN XXIII, Sér. A 2, 251–273.

Nester, P.L., 2008. Basin and Paleoclimate Evolution of the Pampa del Tamarugal Forearc Valley, Atacama Desert, Northern Chile. PhD Thesis (unpublished). Cornell University, Ithaca, New York.

Nester, P.L., Gayo, E., Latorre, C., Jordan, T.E., Blanco, N., 2007. Perennial stream discharge in the hyperarid Atacama Desert of northern Chile during the latest Pleistocene. Proc. Natl. Acad. Sci. 104, 19724–19729. http://dx.doi.org/10.1073/pnas.0705373104.

Osinski, G.R., Kieniewicz, J., Smith, J.R., Boslough, M., Eccleston, M., Scharcz, H.P., Kleindienst, M.R., Haldemann, A.F.C., Churcher, C.S., 2008. The Dakhleh Glass: product of an impact airburst or cratering event in the Western Desert of Egypt? Meteorit. Planet. Sci. 43, 2089–2107. http://dx.doi.org/10.1111/j.1945-5100.2008.tb00663.x.

Osinski, G.R., Schwarcz, H.P., Smith, J.R., Kleindienst, M.R., Haldemann, A.F.C., Churcher, C.S., 2007. Evidence for a ∼200–100 ka meteorite impact in the Western Desert of Egypt. Earth Planet. Sci. Lett. 253, 378–388. http://dx.doi.org/10.1016/j.epsl.2006.10.039.

Pasek, M.A., Block, K., Pasek, V., 2012. Fulgurite morphology: a classification scheme and clues to formation. Contrib. Mineral. Petrol. 164, 477–492. http://dx.doi.org/10.1007/s00410-012-0753-5.

Pigati, J.S., Latorre, C., Rech, J.A., Betancourt, J.L., Martinez, K.E., Budahn, J.R., 2012. Accumulation of impact markers in desert wetlands and implications for the Younger Dryas impact hypothesis. Proc. Natl. Acad. Sci. 109, 7208–7212. http://dx.doi.org/10.1073/pnas.1200296109.

Pigati, J.S., Rech, J.A., Quade, J., Bright, J., 2014. Desert wetlands in the geologic record. Earth-Sci. Rev. 132, 67–81. http://dx.doi.org/10.1016/j.earscirev.2014.02.001.

Placzek, C., Quade, J., Patchett, P.J., 2006. Geochronology and stratigraphy of late Pleistocene lake cycles on the southern Bolivian Altiplano: implications for causes of tropical climate change. Geol. Soc. Am. Bull. 118, 515–532. http://dx.doi.org/10.1130/B25770.1.

Prat-Guitart, N., Rein, G., Hadden, R.M., Belcher, C.M., Yearsley, J.M., 2016. Propagation probability and spread rates of self-sustained smouldering fires under controlled moisture content and bulk density conditions. Int. J. Wildland Fire. http://dx.doi.org/10.1071/WF15103.

Quade, J., Rech, J.A., Betancourt, J.L., Latorre, C., Quade, B., Rylander, K.A., Fisher, T., 2008. Paleowetlands and regional climate change in the central Atacama Desert, Northern Chile. Quat. Res. 69, 343–360. http://dx.doi.org/10.1016/j.yqres.2008.01.003.

Quesada, B., Sylvestre, F., Vimeux, F., Black, J., Paillès, C., Sonzogni, C., Alexandre, A., Blard, P.-H., Tonetto, A., Mazur, J.-C., Bruneton, H., 2015. Impact of Bolivian paleolake evaporation on the δ18O of the Andean glaciers during the last deglaciation (18.5–11.7 ka): diatom-inferred δ18O values and hydro-isotopic modeling. Quat. Sci. Rev. 120, 93–106. http://dx.doi.org/10.1016/j.quascirev.2015.04.022.

Rech, J.A., Pigati, J.S., Quade, J., Betancourt, J.L., 2003. Re-evaluation of mid-Holocene deposits at Quebrada Puripica, Northern Chile. Palaeogeogr. Palaeoclimatol. Palaeoecol. 194, 207–222. http://dx.doi.org/10.1016/S0031-0182(03)00278-5.

Rech, J.A., Quade, J., Betancourt, J.L., 2002. Late Quaternary paleohydrology of the central Atacama Desert (lat 22°–24°S), Chile. Geol. Soc. Am. Bull. 114, 334–348. http://dx.doi.org/10.1130/0016-7606(2002)114<0334:LQPOTC>2.0.CO;2.

Reimold, W.U., Koeberl, C., 2014. Impact structures in Africa: a review. J. Afr. Earth Sci. 93, 57–175. http://dx.doi.org/10.1016/j.jafrearsci.2014.01.008.

Rein, G., Cleaver, N., Ashton, C., Pironi, P., Torero, J.L., 2008. The severity of smouldering peat fires and damage to the forest soil. Catena 74, 304–309. http://dx.doi.org/10.1016/j.catena.2008.05.008.

Roperch, P., Chauvin, A., Lara, L.E., Moreno, H., 2015. Secular variation of the Earth's magnetic field and application to paleomagnetic dating of historical lava flows in Chile. Phys. Earth Planet. Inter. 242, 65–78. http://dx.doi.org/10.1016/j.pepi.2015.03.005.

Sáez, A., Godfrey, L.V., Herrera, C., Chong, G., Pueyo, J.J., 2016. Timing of wet episodes in Atacama Desert over the last 15 ka. The Groundwater Discharge Deposits (GWD) from Domeyko Range at 25°S. Quat. Sci. Rev. 145, 82–93. http://dx.doi.org/10.1016/j.quascirev.2016.05.036.

Schultz, P.H., Harris, R.S., Clemett, S.J., Thomas-Keprta, K.L., Zarate, M., 2014. Preserved flora and organics in impact melt breccias. Geology 42, 515–518. http://dx.doi.org/10.1130/G35343.1.

Schultz, P.H., Zárate, M., Hames, B., Koeberl, C., Bunch, T., Storzer, D., Renne, P., Wittke, J., 2004. The Quaternary impact record from the Pampas, Argentina. Earth Planet. Sci. Lett. 219, 221–238. http://dx.doi.org/10.1016/S0012-821X(04)00010-X.

Shuvalov, V.V., Trubetskaya, I.A., 2007. Aerial bursts in the terrestrial atmosphere. Sol. Syst. Res. 41, 220–230. http://dx.doi.org/10.1134/S0038094607030057.

Sponholz, B., Baumhauer, R., Felix-Henningsen, P., 1993. Fulgurites in the southern Central Sahara, Republic of Niger, and their palaeoenvironmental significance. Holocene 3 (2), 97–104.

Stolper, E., 1982. Water in silicate glasses: an infrared spectroscopic study. Contrib. Mineral. Petrol. 81, 1–17.

Stoof, C.R., Moore, D., Fernandes, P.M., Stoorvogel, J.J., Fernandes, R.E.S., Ferreira, A.J.D., Ritsema, C.J., 2013. Hot fire, cool soil. Geophys. Res. Lett. 40, 1534–1539. http://dx.doi.org/10.1002/grl.50299.

Stracher, G.B., Prakash, A., Sokol, E.V. (Eds.), 2011. Coal and Peat Fires: A Global Perspective, 1st ed.. Elsevier, Amsterdam, Oxford, UK, Boston.

Surovell, T.A., Holliday, V.T., Gingerich, J.A.M., Ketron, C., Haynes, C.V., Hilman, I., Wagner, D.P., Johnson, E., Claeys, P., 2009. An independent evaluation of the Younger Dryas extraterrestrial impact hypothesis. Proc. Natl. Acad. Sci. 106, 18155–18158. http://dx.doi.org/10.1073/pnas.0907857106.

Svensen, H., Dysthe, D.K., Bandlien, E.H., Sacko, S., Coulibaly, H., Planke, S., 2003. Subsurface combustion in Mali: refutation of the active volcanism hypothesis in West Africa. Geology 31, 581. http://dx.doi.org/10.1130/0091-7613(2003)031<0581:SCIMRO>2.0.CO;2.

Svetsov, V., Shuvalov, V., 2008. Tunguska catastrophe of 30 June 1908. In: Adushkin, V., Nemchiniv, I.V. (Eds.), Catastrophic Events Caused by Cosmic Objects. Springer, Berlin, Heidelberg, pp. 227–266.

Sylvestre, F., Servant, M., Servant-Vildary, S., Causse, C., Fournier, M., Ybert, J.-P., 1999. Lake-level chronology on the Southern Bolivian Altiplano (18°–23°s) during late-glacial time and the early Holocene. Quat. Res. 51, 54–66. http://dx.doi.org/10.1006/qres.1998.2017.

Tauxe, L., Staudigel, H., 2004. Strength of the geomagnetic field in the Cretaceous Normal Superchron: new data from submarine basaltic glass of the Troodos Ophiolite. Geochem. Geophys. Geosyst. 5. http://dx.doi.org/10.1029/2003GC000635.

Thellier, E., Thellier, O., 1959. Sur l'intensité du champ magnétique terrestre dans le passé historique et géologique. Ann. Géophys. 15, 285–376.

Van Hoesel, A., Hoek, W.Z., Pennock, G.M., Drury, M.R., 2014. The Younger Dryas impact hypothesis: a critical review. Quat. Sci. Rev. 83, 95–114. http://dx.doi.org/10.1016/j.quascirev.2013.10.033.

Vélain, C., 1878. Etude microscopique des verres résultant de la fusion des cendres de graminées. Bull. Soc. Minéral. Fr. 8, 113–125.

Wasson, J.T., 2003. Large Aerial bursts: an important class of terrestrial accretionary events. Astrobiology 3, 163–179.

Wittke, J.H., Weaver, J.C., Bunch, T.E., Kennett, J.P., Kennett, D.J., Moore, A.M.T., Hillman, G.C., Tankersley, K.B., Goodyear, A.C., Moore, C.R., Daniel, I.R., Ray, J.H., Lopinot, N.H., Ferraro, D., Israde-Alcántara, I., Bischoff, J.L., DeCarli, P.S., Hermes, R.E., Kloosterman, J.B., Revay, Z., Howard, G.A., Kimbel, D.R., Kletetschka, G., Nabelek, L., Lipo, C.P., Sakai, S., West, A., Firestone, R.B., 2013. Evidence for deposition of 10 million tonnes of impact spherules across four continents 12,800 y ago. Proc. Natl. Acad. Sci. 110, E2088–E2097. http://dx.doi.org/10.1073/pnas.1301760110.

Yu, Y., 2011. Importance of cooling rate dependence of thermoremanence in paleointensity determination. J. Geophys. Res. 116. http://dx.doi.org/10.1029/2011JB008388.